

7-19-2016

# CBRS Spectrum Sharing between LTE-U and WiFi: A Multiarmed Bandit Approach

Imtiaz Parvez

*Department of Electrical and Computer Engineering, Florida International University, iparvez@fiu.edu*

M. G. S. Sriyananda

*Department of Electrical and Computer Engineering, Florida International University*

Ismail Guvenc

*North Carolina State University*

Mehdi Bennis

*University of Oulu*

Arif I. Sarwat

*Department of Electrical and Computer Engineering, Florida International University, asarwat@fiu.edu*

Follow this and additional works at: [https://digitalcommons.fiu.edu/ece\\_fac](https://digitalcommons.fiu.edu/ece_fac)



Part of the [Electrical and Computer Engineering Commons](#)

## Recommended Citation

Imtiaz Parvez, M. G. S. Sriyananda, İsmail Güvenç, Mehdi Bennis, and Arif Sarwat, "CBRS Spectrum Sharing between LTE-U and WiFi: A Multiarmed Bandit Approach," *Mobile Information Systems*, vol. 2016, Article ID 5909801, 12 pages, 2016. doi:10.1155/2016/5909801

This work is brought to you for free and open access by the College of Engineering and Computing at FIU Digital Commons. It has been accepted for inclusion in Electrical and Computer Engineering Faculty Publications by an authorized administrator of FIU Digital Commons. For more information, please contact [dcc@fiu.edu](mailto:dcc@fiu.edu).

## Research Article

# CBRS Spectrum Sharing between LTE-U and WiFi: A Multiarmed Bandit Approach

Imtiaz Parvez,<sup>1</sup> M. G. S. Sriyananda,<sup>1</sup> İsmail Güvenç,<sup>2</sup> Mehdi Bennis,<sup>3</sup> and Arif Sarwat<sup>1</sup>

<sup>1</sup>Department of Electrical & Computer Engineering, Florida International University, Miami, FL 33174, USA

<sup>2</sup>Department of Electrical & Computer Engineering, North Carolina State University, Raleigh, NC 27513, USA

<sup>3</sup>Department of Communications Engineering, University of Oulu, 90014 Oulu, Finland

Correspondence should be addressed to Arif Sarwat; [asarwat@fiu.edu](mailto:asarwat@fiu.edu)

Received 31 March 2016; Revised 14 June 2016; Accepted 19 July 2016

Academic Editor: Miguel López-Benítez

Copyright © 2016 Imtiaz Parvez et al. This is an open access article distributed under the Creative Commons Attribution License, which permits unrestricted use, distribution, and reproduction in any medium, provided the original work is properly cited.

The surge of mobile devices such as smartphone and tablets requires additional capacity. To achieve ubiquitous and high data rate Internet connectivity, effective spectrum sharing and utilization of the wireless spectrum carry critical importance. In this paper, we consider the use of unlicensed LTE (LTE-U) technology in the 3.5 GHz Citizens Broadband Radio Service (CBRS) band and develop a multiarmed bandit (MAB) based spectrum sharing technique for a smooth coexistence with WiFi. In particular, we consider LTE-U to operate as a General Authorized Access (GAA) user; hereby MAB is used to adaptively optimize the transmission duty cycle of LTE-U transmissions. Additionally, we incorporate downlink power control which yields a high energy efficiency and interference suppression. Simulation results demonstrate a significant improvement in the aggregate capacity (approximately 33%) and cell-edge throughput of coexisting LTE-U and WiFi networks for different base station densities and user densities.

## 1. Introduction

Due to the proliferation of mobile devices and diverse mobile applications, the exponentially increasing mobile data is doubled approximately every year [1]. The 4G Long-Term Evolution (LTE) has recently emerged as a powerful technology to provide broadband data rates. On the other hand, to satisfy the throughput demand of broadband LTE networks in the upcoming years, larger bandwidth is needed [2, 3]. Since the licensed spectrum is expensive and limited, extending the operation of LTE in the underutilized unlicensed bands is recently getting significant attention, which requires effective coexistence with other technologies such as WiFi in these bands.

Recently, the Federal Communications Commission (FCC) in the United States has been working on opening a 150 MHz of spectrum in the 3.5 GHz band for sharing among multiple technologies, which is also commonly referred to as the Citizen Broadband Radio Service (CBRS). However, the use of this spectrum is subject to regularity requirements, where the incumbent military and meteorological radar

systems have to be protected [4, 5]. In the CBRS band, there are three kinds of users with hierarchical priority: Incumbent Access (IA) users (tier-1), Prioritized Access License (PAL) users (tier-2), and General Authorized Access (GAA) users (tier-3) as illustrated in Figure 1. In the current scenario, the expansion of unlicensed LTE (LTE-U) as PAL or GAA user in the CBRS band is an enticing choice because of high penetration at 3.5 GHz, clean channel, and wide amount of spectrum [6]. The Third-Generation Partnership Project (3GPP) standardization group has been recently working on standardizing the licensed-assisted access (LAA) technology in the 5 GHz spectrum [7, 8]. The main goal is to develop a global single framework of LAA of LTE in the unlicensed bands, where operation of LTE will not critically affect the performance of WiFi networks in the same carrier. In the initial phase, only downlink (DL) operation LTE-A (LTE Advanced) Carrier Aggregation (CA) in the unlicensed band was considered, while deferring the simultaneous operation of DL and uplink (UL) to the next phase.

Another option for the operation of LTE in the unlicensed spectrum is through a prestandard approach, referred to

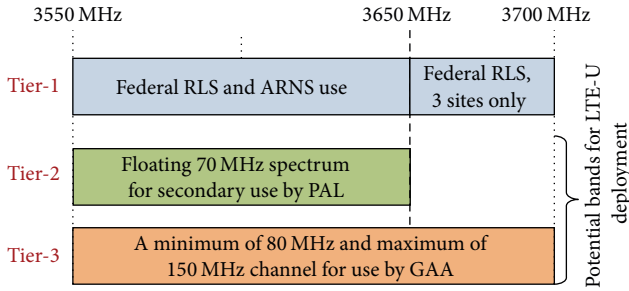


FIGURE 1: CBRS spectrum with 3 types of users.

LTE-U, where LTE base stations leave transmission gaps for facilitating coexistence with WiFi networks. Development of LTE-U technology is led by the industry consortium known as the LTE-U Forum. LTE-U mainly focuses on the operation of unlicensed LTE in the regions (e.g., USA, China) where listen before talk (LBT) is not mandatory. LTE-U defines the operation of primary cell in a licensed band with one or two secondary cells (SCells), each 20 MHz in the 5 GHz unlicensed band: U-NII-1 and/or U-NII-3 bands, spanning 5150–5250 MHz and 5725–5825 MHz, respectively. However, both the LTE-U and LAA need licensed band for control plane. Similar to the 5 GHz band, CBRS band can be utilized for LTE-U operation in the absence of IA users such as radar signal.

In our study, we consider the coexistence problem of LTE-U and WiFi networks in the CBRS bands. Since WiFi adopts a contention based medium access control with random back-off [9] for channel access and LTE uses dynamic scheduling for users, the unrestrained LTE operation in the same band will generate continuous interference on WiFi service. To operate LTE-U and WiFi simultaneously in the same unlicensed spectrum, fair and reasonable coexistence mechanism is indispensable. The adverse impact on DL and UL WiFi transmissions due to LTE deployment in the same band is analyzed in [10–12], emphasizing the need for rigorous studies. In this regard, discrete mechanisms such as dynamic channel selection, retaining transmission gaps, transmission duty cycle manipulation, and LBT have been proposed in the literature for harmonious coexistence with improved performance. To select resources dynamically, learn from the environment, and adaptively modify transmission parameters for performance improvement, various machine learning based techniques [13–16] have been introduced.

In this paper, we introduce a reinforcement learning (MAB) based adaptive duty cycle selection for the coexistence between LTE-U and WiFi. Multiarmed Bandit (MAB) is a machine learning technique designed to maximize the long-term rewards through learning provided that each agent is rewarded after pulling an arm. Basically MAB [17, 18] problem resembles a gambler (agent) with a finite number of slot machines in which the gambler wants to maximize his rewards over a time horizon. Upon pulling an arm, a reward is attained with prior unknown distribution. The goal is to pull arms sequentially so that the accumulated rewards over the gambling period are maximized. However, the problem

involves the exploration versus exploitation trade-off, that is, taking actions to yield immediate higher reward on the one hand and taking actions that would give rewards in the future, on the other hand.

In our technique, we use a multiarm bandit (MAB) algorithm for selecting appropriate duty cycle. Using a 3GPP compliant Time Division Duplex- (TDD-) LTE and Beacon enabled IEEE 802 systems in the 3.5 GHz band, we simulate and evaluate the coexistence performance for different percentage of transmission gaps. We found a significant throughput improvement for both systems ensuring harmonious coexistence. The objectives, subsequently the gains, of this study are not limited to throughput enhancements. The benefits that are achieved in different dimensions with the aid of MAB scheme and the other supporting techniques like PC can be summarized as follows:

- (1) Proper coexistence is achieved due to the dynamic exploring and exploitation by MAB. So our technique is adaptive.
- (2) The aggregate capacity is improved. Due to the application of MAB algorithm, optimal or suboptimal solutions are achieved.
- (3) Using DL PC higher capacity values are achieved under dense UE and STA configurations.
- (4) Higher energy efficiency is also achieved with PC, which always attempts to reduce the transmission power while increasing the energy efficiency.
- (5) With the use of learning algorithm, a high degree of efficiency is achieved.

To the best of our knowledge, our work is the first study that introduces MAB for improving the coexistence of LTE and WiFi in the unlicensed bands.

The rest of the paper is organized as follows. Section 2 provides a literature review of coexistence of LTE-U and WiFi. In Section 3, we provide our system model and problem formulation for LTE and WiFi coexistence. Section 4 introduces the proposed MAB based dynamic duty cycle selection approach. Simulation results with various parameter configurations are presented in Section 5. Finally, Section 6 provides concluding remarks.

## 2. Related Works

*2.1. Coexistence among Unlicensed LTE and WiFi.* In the literature, several studies can be found that investigate the performance of LTE and WiFi coexistence in the unlicensed bands. In [19], coexistence performance of LTE and WiFi has been investigated in 900 MHz considering single floor and multifloor indoor office scenarios. It is shown that the performance of WiFi is heavily affected when WiFi and LTE operate simultaneously in the unlicensed spectrum.

To facilitate harmonious coexistence between LTE-U and WiFi in the same band, mainly three techniques have been proposed in the literature: (1) listen before talk (LBT), (2) dynamic channel selection, and (3) coexistence gaps. In Europe and Japan, LBT is mandatory for data offloading in

unlicensed band. The usage of LBT has been justified in [20] with different choice of LBT schemes. In [21], LBT is presented considering interratio access technology (RAT) and intra-RAT. In this technique, energy detection based LBT is proposed to handle inter-RAT interference whereas cross correlation based LBT is used to handle intra-RAT interference. However, LBT is not mandatory in USA and China, where alternative coexistence techniques can be explored.

In [22], Qualcomm presents an effective channel selection policy based on interference level. If the interference of the occupied channel exceeds a certain level, LTE-U changes the channel, provided that the interference is measured before and during the operation, and both at the user equipment (UE) and the network side. On the other hand, in [6] adaptive bandwidth channel allocation offered by LTE and Least Congested Channel Search (LCCS) has been suggested for channel selection. Dynamic channel selection requires free or low-interference channel to utilize. Since same band will be shared by other cellular service providers as well as different technologies such as WiFi, finding of clean channel may not be practical.

In [23], blank subframe allocation by LTE has been proposed where LTE is restrained from transmitting, and WiFi keeps on transmission. A similar technique has been proposed in [24] where certain subframes of LTE-U are reserved for WiFi transmission. Qualcomm has proposed Carrier Sensing Adaptive Transmission (CSAT) [22] for LTE-U MAC scheduling in which a fraction of TDD duty cycle is used for LTE-U transmission and the rest is used for other technologies. The cyclic ON/OFF ratio can be adaptively adjusted based on the activity of WiFi during the OFF period. In this paper, we focus on the dynamic optimization of coexistence gap/transmission time along with DL power control.

Uplink (UL) power control has been investigated on the performance of LTE-WiFi coexistence in [25, 26]. However, DL power control in coexistence problem has not been explored yet considering uncoordinated LTE and WiFi systems. The DL power control enhances performance by reducing interferences, which is demonstrated in [27–29]. In our study, we optimize both the transmission time and DL power using machine learning technique.

Reinforcement algorithm such as Q-learning, multiarm bandit, and value iteration is effective variant of machine learning which has been applied for optimization problems of cellular systems such as channel selection, mobility management, resource allocation, and rate adoption. In [13], Q-learning based duty cycle adjustment is presented to facilitate the sharing of the channel and to increase the overall throughput. In [30], a MAB based distributed channel selection is proposed to use vacant cellular channels in device to device (D2D) communication. To enhance handover process and increase throughput, MAB techniques based context-aware mobility management scheme is studied in [31]. In [32], dynamic rate adaptation and channel selection from free primary users have been proposed in cognitive radio systems using MAB, which yields extensive throughput improvements.

In our study, we propose a MAB based dynamic duty cycle selection for unlicensed LTE systems. In particular, LTE base

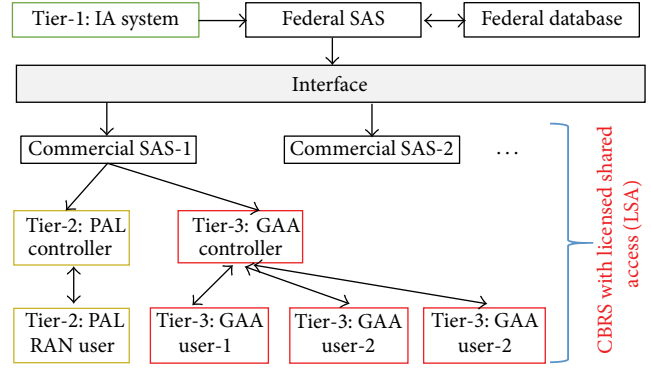


FIGURE 2: Users access priority.

stations (BSs) measure the utilization of the channel based on channel status information (CSI), learn the channel utilization of WiFi (current and previous), select the optimum duty cycle and transmission power, and perform transmission under this duty cycle, which results in effective sharing of wireless spectrum with WiFi networks. Due to this dynamic learning, our technique is adaptive and it improves aggregate capacity and energy efficiency. This is the first time we are applying MAB for coexisting operation of LTE and WiFi.

**2.2. CBRS Spectrum Sharing.** The CBRS spectrum is composed of 150 MHz bandwidth divided into two chunks: 80 MHz and 70 MHz. Based on the architecture of CBRS band, the spectrum users are prioritized into three groups with decreasing interference protection requirements as illustrated in Figure 2.

The IA users in tier-1, such as military radars, have the most protection, mainly through geographical *exclusion zones* [33] that averts other users from transmitting in the vicinity of IA users. While the NTIA in April 2015 [5, 34] shrunk the earlier exclusion zones in [33] by 77%, they still cover several of the Nation's largest cities [35]. The main challenge of PAL users in tier-2 have is to protect the IA users and other PAL users from interference. To facilitate this, a spectrum access system (SAS) [36] is utilized, which grants spectrum access to users based on their locations. The network providers can purchase PAL licenses in given geographical areas, which consist of census tracts. Up to a 70 MHz of PAL spectrum will be available, with chunks of 10 MHz channels, which will be auctioned if there is more demand from providers than the available spectrum. Finally, tier-3 users are GAA users which are allowed to operate in the spectrum that are not used by IA and PAL tiers. In areas with no IA and PAL activity, GAA users may have access to whole 150 MHz, while in areas with PAL activity but outside of IA exclusion zones, at least 80 MHz of bandwidth will always be available for GAA use.

Since spectrum is limited and expensive, wireless service provider (LTE, WiFi) will be interested to operate in CBRS band as GAA users. In the GAA band, LTE needs to coexist with other cellular operators as well as other technologies such as WiFi. Besides that, Licensed Shared Access (LSA) concept [37, 38] allows an incumbent spectrum user to share

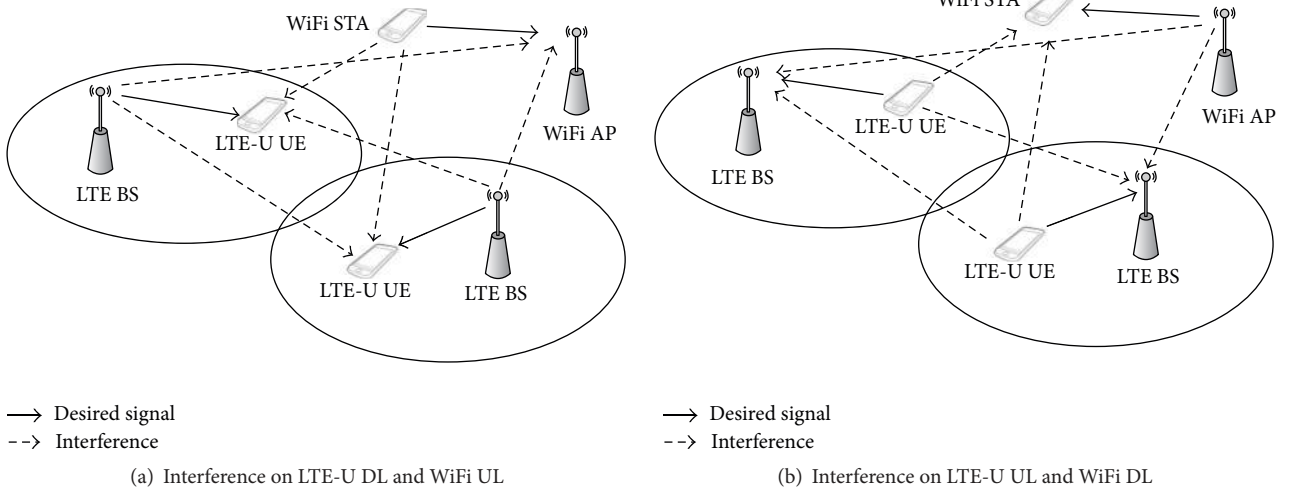


FIGURE 3: DL and UL interference scenarios for LTE-U/WiFi transmissions.

spectrum with licensed users with defined rights to access a portion of spectrum at a given location and time. This also requires to develop coexistence mechanism between mobile network operators (MNOs) and other technologists (licensed/unlicensed) such as WiFi. In this study, we focus on the coexistence of LTE and WiFi in the 3.5 GHz CBRS spectrum. For this study, for simplicity, we assume that the coexistence with IA and PAL users are already maintained through a SAS database, and we only consider coexistence among LTE-U and WiFi users in the GAA bands.

### 3. System Model and Problem Formulation

To evaluate the coexistence performance of LTE-U with WiFi in the unlicensed band, a collocated LTE-U and WiFi network scenario is considered. The sets of LTE-U BSs, WiFi APs, LTE-U UEs for BS  $i$ , and WiFi STAs for AP  $w$  are given by  $\mathcal{B}_L$ ,  $\mathcal{B}_W$ ,  $\mathcal{Q}_L^i$ , and  $\mathcal{Q}_W^w$ , respectively.  $\mathcal{Q}_L = \{\mathcal{Q}_L^1, \mathcal{Q}_L^2, \dots, \mathcal{Q}_L^i, \dots, \mathcal{Q}_L^{|\mathcal{B}_L|}\}$  and  $\mathcal{Q}_W = \{\mathcal{Q}_W^1, \mathcal{Q}_W^2, \dots, \mathcal{Q}_W^w, \dots, \mathcal{Q}_W^{|\mathcal{B}_W|}\}$  represent the sets of all UEs and STAs. For LTE-U, TDD-LTE is considered. For synchronization of WiFi STAs with the corresponding APs, a periodic beacon transmission is used as in [13].

**3.1. Interference on DL and UL Transmissions.** Interference caused to LTE-U UE and LTE-U BS during DL and UL transmissions is shown in Figure 3. A TDD frame structure similar to that in [39, Figure 6.2] is considered for all the BSs and UEs with synchronous operation. As shown in Figure 3(a), in the simultaneous operation of an LTE-U within a WiFi coverage area, the DL LTE-U radio link experiences interference from other LTE-U DL and WiFi UL transmissions. As the same time, WiFi UL suffers from near LTE-U transmission. During an UL transmission subframe, shown in Figure 3(b), LTE-U BS is interfered by the UL transmission of LTE-U UEs, as well as the DL transmissions of WiFi. Similarly, WiFi DL transmission is interfered by other LTE-U ULs where the DL received signal of a WiFi STA is interfered by other LTE-U UL transmissions. In the coexistence scenarios with

high density of WiFi users, WiFi transmissions get delayed degrading their capacity performance due to the use of carrier sense multiple access with collision avoidance (CSMA/CA) mechanism [40]. This is an additional degradation other than the performance reduction experienced due to LTE-U transmissions operated on the same spectrum and this is valid only for WiFi APs and STAs.

**3.2. Duty Cycle of LTE-U.** In the case of designing a duty cycle for LTE-U, multiple LTE TDD frames are considered. For that purpose, five consecutive LTE frames [39, Figure 6.2(a)] are used to construct a duty cycle. Similar to [13], the LTE-U transmission ON/OFF condition is used to define a duty cycle which is shown in Figure 4 (e.g., 40% duty cycle: during the first two consecutive LTE-U frames, transmission is turned on and it is turned off during the following three frames). One out of these two configurations is used by the UEs and BS in an LTE cell during a duty cycle period. According to this structure, a constant UL:DL duty cycle value is maintained.

**3.3. Capacity Calculation and Power Control.** For any BS  $i \in \mathcal{Q}_L$ , there are  $\mathcal{N}^i$  resource blocks (RBs) for the DL. For a given UE  $u$  associated with BS  $i$ ,  $n_u^i$  RBs are allocated, where  $\mathcal{N}^i = \sum_{u=1}^{|\mathcal{Q}_L^i|} n_u^i$ .  $p_{s,r}^i$ ,  $p_{s,r}^b$ ,  $p_{s,r}^a$ , and  $p_{s,r}^q$  are transmit power values associated with RB  $r$  and the transmit power index  $s$  from the LTE-U BS  $i$ , LTE-U BS  $b$  ( $i \neq b$ ), WiFi AP  $a$ , and WiFi STA  $q$ .  $i$ th BS is considered as the desired BS where the BSs indexed by  $b$  are the interference generating BSs. For any AP, UE, or STA total transmit power is equally distributed among all RBs. However, in every BS, the total transmit power is dynamically changed for every duty cycle according to MAB algorithm.  $h_{u,r}^i$ ,  $h_{u,r}^b$ ,  $h_{u,r}^a$ , and  $h_{u,r}^q$  are the channel gain values from BS  $i$  to UE  $u$ , from BS  $b$  to UE  $u$ , from AP  $a$  to UE  $u$ , and from WiFi STA  $q$  to UE  $u$ , respectively. All channel gain values are calculated considering path losses and shadowing. In that case, interference generated to UE  $u$  from BSs, APs, and STAs are given by  $I_{BS}^u$ ,  $I_{AP}^u$ , and  $I_{STA}^u$ , respectively. Since a synchronized transmission is considered,

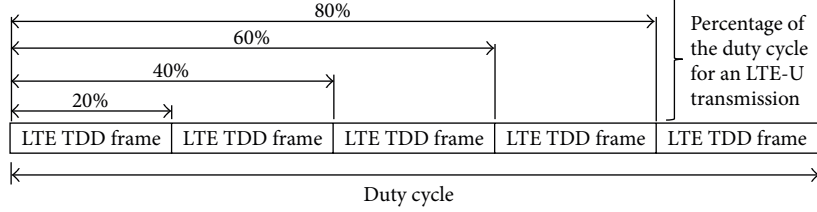


FIGURE 4: Structure of the duty cycle for LTE-U transmissions.

there is no interference from the UL transmission of LTE-U UEs. Noise variance is denoted by  $\sigma^2$ . The Signal-to-Interference-plus-Noise Ratio (SINR) expression for UE  $u$  served by BS  $i$  on RB  $r$  at time interval  $k$  is given as

$$\text{SINR}_{u,r}^i [k] = \frac{p_s^i h_{u,r}^i}{\underbrace{\sum_{b \in \mathcal{B}_L \setminus i} p_s^b h_{u,r}^b}_{I_{\text{BS}}^u} + \underbrace{\sum_{a \in \mathcal{B}_W} p_s^a h_{u,r}^a}_{I_{\text{AP}}^u} + \underbrace{\sum_{q \in \mathcal{Q}_W} p_s^q h_{u,r}^q}_{I_{\text{STA}}^u} + \sigma^2}, \quad (1)$$

where  $b, i \in \mathcal{B}_L$ .

The amount of successfully transmitted data bits  $N_B$  from  $i$ th LTE-U BS during  $T_{\text{OFDM}}$  time interval  $k$  within an active DL subframe/s of a duty cycle is given by

$$N_B^i = \sum_k \sum_{u \in \mathcal{Q}_L^i} \sum_r^{R_u} W_{u,r}^i \log_2 (1 + \text{SINR}_{u,r}^i [k]) T_{\text{OFDM}}, \quad (2)$$

where  $T_{\text{OFDM}}$  is the orthogonal frequency division multiplexing (OFDM) symbol duration,  $T_{\text{Tx}}^i = \mathcal{K}^i T_{\text{OFDM}}$ , and  $\mathcal{K}^i$  is the total number of transmit  $T_{\text{OFDM}}$  time intervals for the considered duty cycle. The total allocated bandwidth for RB  $r$  for UE  $u$  served by BS  $i$  is  $W_{u,r}^i$ . The average capacity over a duty cycle period is used as a performance measure in this study as in [13]. The DL capacity  $C_i$  of LTE-U BS  $i$  is given as

$$C_i = \frac{N_B^i}{T_{\text{Tx}}^i + T_{\text{Wait}}^i}, \quad (3)$$

where  $T_{\text{Wait}}^i$  is the waiting time due to silent subframe allocation.

The capacity  $C_i$  in (3) is used as a performance measure for each LTE-U BS. Since the transmit power of one BS contributes to the interference power of the other BS, neighboring BSs are coupled in terms of interference. The goal of every BS is to maximize  $C_i$  while minimizing the DL transmit power  $p_s^i$ ,  $\forall i \in \mathcal{B}_L$ . By minimizing the transmit power values  $p_s^i$  and  $p_s^b$ , the goal is to achieve a comparatively higher energy efficiency than the case of constant DL transmit power. In the same time a reduction in interference is also expected while guaranteeing a minimum capacity. Moreover,  $P_{\min} \leq p_s^b \leq P_{\max}$ , where  $P_{\min}$  and  $P_{\max}$  are the minimum and maximum transmit power constraints, respectively. The minimum capacity corresponding to a given action is denoted by

$C_j^{\min}$ . The objective is to maximize the average capacity while minimizing the transmit power, which can be written as

$$\text{maximize} \quad \frac{\sum_{i=1}^{|\mathcal{B}_L|} C_i}{|\mathcal{B}_L|} \quad (4)$$

$$\text{minimize} \quad p_s^i \quad \forall i \in \mathcal{B}_L \quad (5)$$

$$\text{subject to} \quad \{p_s^i, p_s^b\} \leq P_{\max}, \quad (6)$$

$$\forall i, b \in \mathcal{B}_L, i \neq b, s \in S$$

$$\{p_s^i, p_s^b\} \geq P_{\min}, \quad (7)$$

$$\forall i, b \in \mathcal{B}_L, i \neq b, s \in S$$

$$C_i > C_j^{\min}, \quad \forall i \in \mathcal{B}_L, \forall j \in J. \quad (8)$$

In the case of energy efficiency, several parameter configurations are considered for (8) as

$$\frac{C_i}{p_s^i} > \frac{C_j^{\min}}{p_s^j},$$

$$\text{or} \quad \frac{C_i}{p_s^i} > \frac{C_j^{\min}}{P_{\min}}, \quad (9)$$

$$\text{or} \quad \frac{C_i}{p_s^i} > \frac{C_j^{\min}}{P_{\max}}.$$

Due to the same denominator,  $C_i/p_s^i > C_j^{\min}/p_s^j$  is simplified to (8), which can be used as a proportional measure of energy efficiency. The problem is reformulated defining a new objective to maximize energy efficiency as follows:

$$\text{maximize} \quad \frac{\sum_{i=1}^{|\mathcal{B}_L|} (C_i/p_s^i)}{|\mathcal{B}_L|} \quad (10)$$

$$\text{subject to} \quad (6), (7) \text{ and } (9).$$

#### 4. MAB Techniques for LTE-U WiFi Coexistence

In a MAB problem, an agent selects an action (also known as arm) and observes the corresponding reward. The rewards for given action/arms are random variables with unknown distribution. The goal of MAB is to design action selection

```

(1) Initialization:
(2) Set the minimum capacity values  $C_j^{\min}$ ,  $\forall j \in J$ , Exploration steps  $M$ , Beta  $(1, 1)$ ,  $\alpha_j^i$  and  $\beta_j^i$  where  $\forall j: j \in J$ .
   Select  $d_j^i$ ,  $\forall j \in J$ , update  $s$ ,  $n_{i,0}(d_j^i)$ ,  $v_{i,0}(d_j^i)$  and accumulated hypothesis/reward  $R_i(d_j^i)$  based on  $C_i > C_j^{\min}$ 
(3) if  $\alpha_j^i(m) = \beta_j^i(m)$ ,  $\forall (l, m) \in M$  then
(4)   Exploration:
(5)   for  $m = 1, 2, 3, \dots, M$  do
(6)     Select  $d_j^i, d_j^i \in \mathcal{D}_i$ ,  $j \in \{\mathcal{U}(1, |\mathcal{D}_i|) \cap J\}$  and update  $s$ , (8)
(7)     Execute  $\{d_j^i, p_s^i\}$ , observe  $C_i$  and update  $n_{i,m}(d_j^i)$ 
(8)     if  $C_i > C_j^{\min}$  then
(9)       Reward,  $R_i(d_j^i) = R_i(d_j^i) + 1$ 
(10)      Update  $s$  ( $s \leftarrow s - 1$ ) and  $v_{i,m}(d_j^i)$ , (11)
(11)      Update  $\alpha_j^i(m) = \alpha_j^i(m) + 1$ 
(12)     else
(13)       Reward,  $R_i(d_j^i) = R_i(d_j^i) + 0$ 
(14)       Update  $s$  ( $s \leftarrow s + 1$ ) and  $v_{i,m}(d_j^i)$ , (11)
(15)       Update  $\beta_j^i(m) = \beta_j^i(m) + 1$ 
(16)     end if
(17)   if  $R_i(d_j^i) = R_i(d_a^i)$ ,  $d_j^i, d_a^i \in \mathcal{D}_i$ ,  $j \neq a$ ,  $\forall j, a \in J$ 
then
(18)     Select  $d_k^i, d_k^i \in \mathcal{D}_i$ ,  $k \in \{\mathcal{U}(1, |\mathcal{D}_i|) \cap J\}$ 
(19)     else
(20)       Select  $d_k^i$ , (12)
(21)     end if
(22)   Exploitation:
(23)   for  $l = 1, 2, 3, \dots, L$  do
(24)     Execute the action  $\mathcal{A}_i = \{d_k^i, p_s^i\}$ 
(25)   end for
(26) end for
(27) end if

```

ALGORITHM 1: Multiarm bandit (Thomson sampling).

strategies to maximize accumulate rewards over a given time horizon. However, the strategies need to achieve a trade-off between exploration (selection of suboptimal actions to learn their average rewards) and exploitation (selection of actions which have provided maximum rewards so far).

In order to dynamically optimize LTE-U transmission parameters (i.e., duty cycle and transmit power), a variant of MAB learning techniques, called Thomson sampling [41, 42] algorithm, is applied. The scenario is formulated as a multiagent problem  $\mathcal{G} = \{\mathcal{B}_L, \{\mathcal{A}_i\}_{i \in \mathcal{B}_L}, \{C_i\}_{i \in \mathcal{B}_L}\}$ , considering the BSs as players, where  $\mathcal{A}_i$  is the action set for player  $i$ . During the entire process, each BS needs to strike a balance between exploration and exploitation, where there are  $M$  exploration and  $L$  exploitation steps, indexed with  $m$ ,  $1 \leq m \leq M$ , and  $l$ ,  $1 \leq l \leq L$ , respectively.

(i) *Agents.* LTE-U BSs,  $\mathcal{B}_L$ .

(ii) *Action.* The action set of agent  $i$ ,  $\mathcal{A}_i$  is defined as  $\mathcal{A}_i = \{d_j^i, p_s^i\}_{j \in J, s \in S}$ .  $\{d_j^i, p_s^i\}$  is the pair of duty cycle and transmit power elements. Configurations of duty cycles are used as part of the action space  $\mathcal{D}$ , where  $\mathcal{D}$  is common for all players. A given BS  $i$  selects  $d_j^i, d_j^i \in \mathcal{D}$  according to Algorithm 1 where  $J = \{1, 2, \dots, |\mathcal{D}|\}$ ,  $j \in J$  and  $J \in \mathbb{Z}^+$ . Probability spaces of positive

integers are denoted by  $\mathbb{Z}^+$ . The set of first elements of the action vector  $\mathcal{D}_i = \{d_1^i, d_2^i, \dots, d_{|\mathcal{D}_i|}^i\}$  of BS  $i$  is associated with the duty cycles as  $\{20\%, 40\%, \dots, 80\%$ , respectively. The transmit power values set  $\mathcal{P}$  is represented as  $S = \{1, 2, \dots, |\mathcal{P}|\}$ ,  $s \in S$ , and  $S \in \mathbb{Z}^+$ .  $p_s^i$  is the transmit power of player  $i$ , where  $\mathcal{P}_i = \{p_1^i, p_2^i, \dots, p_{|\mathcal{P}_i|}^i\}$ . For each action  $\mathcal{A}_i$ , there is a distribution Beta  $(\alpha_j^i, \beta_j^i)$ ,  $\forall j \in J$ , where  $\alpha_j^i$  and  $\beta_j^i$  are the shape parameter. However, in the case of power control (PC), if  $C_i > C_j^{\min}$ ,  $s$  is decreased by one ( $s \leftarrow s - 1$ ) reducing the transmit power  $p_s^i$  by one level for the next step  $m + 1$  and vice versa. Further, when  $C_i > C_j^{\min}$  a reward is achieved. And, for  $C_i > C_j^{\min}$ ,  $\alpha_j^i$  is incremented; otherwise,  $\beta_j^i$  is incremented.

(iii) *Decision Function.* The DL capacity of a BS  $i$ ,  $C_i$  is used as the utility function. In order to select a duty cycle, a decision function based on the policy UCBl [43] is used where the accumulated rewards achieved due to values given by  $C_i$  are exploited. The decision value for the duty cycle  $d_j^i$  related to the exploration

step  $m$  of BS  $i$ ,  $v_{i,m}(d_j^i)$ , is given in (11) while  $d_k^i$  based on the decision is given in (12):

$$v_{i,m}(d_j^i) = \bar{x}_{i,m}(d_j^i) + \sqrt{\frac{2 \ln(m + |\mathcal{D}_i|)}{n_{i,m}(d_j^i)}}, \quad (11)$$

$$d_k^i = \arg \max_{d_j^i \in \mathcal{D}_i} (v_{i,m}(d_j^i)), \quad (12)$$

where  $\bar{x}_{i,m}(d_j^i) = R_i(d_j^i)/n_{i,m}(d_j^i)$ . The argument of the maximum value is given by  $\arg \max(\cdot)$ .  $\bar{x}_{i,m}(d_j^i)$ ,  $R_i(d_j^i)$ , and  $n_{i,m}(d_j^i)$  are the average reward obtained from  $d_j^i$  during the exploration step  $m$ , total rewards gained from the same  $d_j^i$ , and the total number of times  $d_j^i$  has been played, respectively. Selection of  $s$  is totally independent of the decision function.

The multiagent learning problem is addressed using a MAB approach. In the contextual MAB problem handled by the Thomson sampling algorithm [41], current and previous information (i.e., history) is used for the selection of an arm or action. Initially  $d_j^i, \forall j \in J$ , are played once with  $p_s^i = p_{|\mathcal{D}_i|}^i$ . Based on the accumulated reward  $R_i(d_j^i)$ , the parameters  $s, n_{i,0}(d_j^i)$ , and  $v_{i,0}(d_j^i)$  are updated. In the learning process, the accumulated reward is used to play the role of the accumulated hypothesis defined in [44]. Subsequently, agents balance between  $M$  exploration and  $L$  exploitations steps. During the exploration steps,  $d_j^i$  is selected randomly, where  $d_j^i, d_k^i \in \mathcal{D}_i, j \in \{\mathcal{U}(1, |\mathcal{D}_i|) \cap \mathcal{I}\}$ , where a uniform distribution with the minimum and maximum values  $x_1$  and  $x_2$  is given by  $\mathcal{U}(x_1, x_2)$ .  $s$  is decided based on the last available values of (8). Subsequently the same set of parameters is updated. At the end of each exploration step, based on (8) and the accumulated rewards an action is selected. Then the same action is repeatedly played for all the  $L$  exploitation steps of that particular exploration step as explained in Algorithm 1.

## 5. Simulation Results

For LTE-U, TDD-LTE is considered and it is assumed that all LTE-U UEs are synchronized in both time and frequency domain as in [13] with the serving BSs. A beacon is transmitted periodically for the purpose of synchronization of WiFi STAs with the corresponding APs. To evaluate the performance, an architecture containing two independently operated layers of cellular deployments is considered as shown in Figure 5. Hexagonal cells with omnidirectional antennas are assumed. LTE-U layer encompasses  $|\mathcal{B}_L| = 7$  BSs and  $|\mathcal{Q}_L|$  UEs, where the WiFi layer includes  $|\mathcal{B}_W| = 7$  APs and  $|\mathcal{Q}_W|$  WiFi STAs. In each cell, for each AP/BS, STAs/UEs are dropped at random locations. All of them are assumed to be uniformly distributed within the cells of their serving BSs having a mobility speed of 3 km/h and a random walk mobility model. We consider a nonfull buffer traffic for both WiFi and LTE networks, where the packet arrivals at the transmitter queues follow a Poisson distribution. The traffic

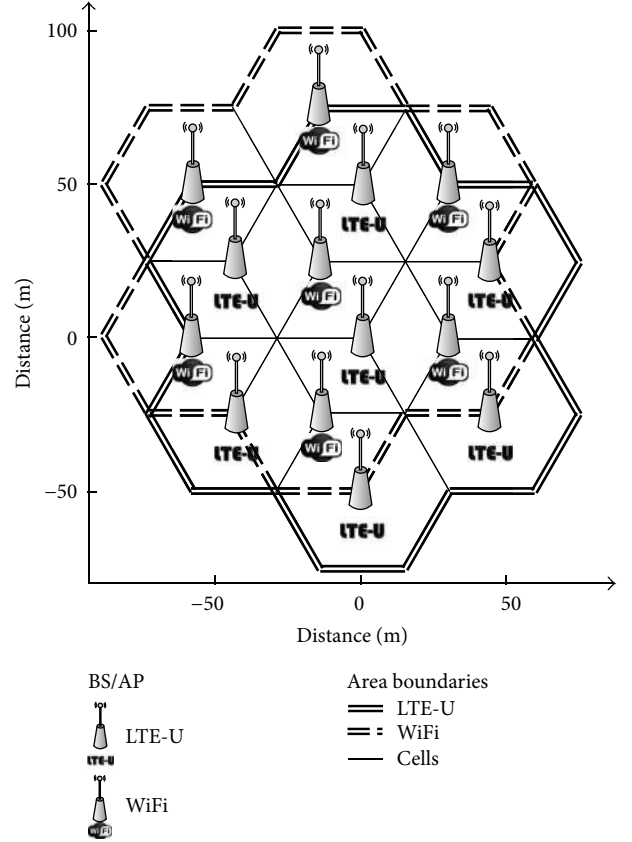


FIGURE 5: Cellular coverage layout used in LTE-U and WiFi coexistence simulations.

arrival rates for LTE-U and WiFi are  $\lambda_{\text{LTE}} = \lambda_{\text{WiFi}} = 2.5$  packet/second.

The LTE and WiFi IEEE 802.11n medium access control (MAC) and physical (PHY) layers are modeled in which a PHY layer abstraction is used for Shannon capacity calculations of WiFi and LTE-U. The time granularity of each WiFi OFDM symbol duration is  $4 \mu\text{s}$ , which we use to periodically capture the number of successfully received bits [13]. For both technologies wireless channel is modeled according to [45], when the systems are operated in the 3.5 GHz band. Indoor Hotspot (InH) scenario is considered with path loss and shadowing parameters. FTP Traffic Model-2 [45] is employed for either WiFi or LTE-U with a noise spectral power density of  $-95 \text{ dBm/Hz}$ .

In each transmission time interval (TTI), DL SINR is reported to the corresponding BS. Based on the number of LTE-U UEs waiting and requesting UL transmission during one subframe, bandwidth is equally shared among themselves. The simulation parameters for LTE-U transmissions are summarized in Table 1. TDD configuration 1 [39, Figure 6.2(a)] is used for the LTE-U frames having a 50 ms total duty cycle period. Minimum required capacity level  $C_j^{\min}$  is 10 Mbps and the set of power levels is  $\mathcal{P}_i = \{p_1^i, p_2^i, \dots, p_{|\mathcal{D}_i|}^i\} = \{8, 13, 18, 23\} \text{ dBm}$ .

For WiFi, CSMA/CA with enhanced distributed channel access (EDCA) and clear channel assessment (CCA) has been



TABLE 1: LTE MAC/PHY parameters.

Parameter	Value
Frequency	3.5 GHz
Transmission scheme	OFDM
Bandwidth	20 MHz
DL Tx power	23 dBm
UL Tx power	PL Based TPC
Frame duration	10 ms
Scheduling	Round Robin
UL base power level $P_0$	-106 dBm
TTI	1 ms

TABLE 2: WiFi MAC/PHY parameters.

Parameter	Value
Frequency	3.5 GHz
Transmission scheme	OFDM
Bandwidth	20 MHz
DL/UL Tx power	23 dBm
Access category	Best effort
MAC protocol	EDCA
CCA channel sensing threshold	-82 dBm
CCA energy detection threshold	-62 dBm
No of service bits in PPDU	16 bits
No of tail bits in PPDU	12 bits
Backoff type	Fixed contention window
Contention window size	$\mathcal{U}(0, 31)$
Noise figure	6 [39]
Beacon interval	100 ms
Beacon OFDM symbol detection threshold	10 dB
Beacon error ratio threshold	15

implemented. All WiFi STAs with traffic in their queue will compete for channel access after receiving a beacon transmission. Without reception of a signal beacon, transmission or reception will not be initiated. The WiFi STA will sense the channel and will transmit if it is idle. Otherwise, transmission will be backed off and the next transmission will be initiated after a backoff time. Random backoff time mechanism is used for this study. All the parameters for the WiFi transmission are summarized in Table 2.

**5.1. Aggregate Capacity with MAB.** Aggregate capacity of stand-alone WiFi, coexisting LTE-U (80% duty cycle) and WiFi (with no MAB algorithm), and MAB based coexistence of LTE-U and WiFi are presented in Figure 7. The aggregate numbers of WiFi APs and LTE BSs in all scenarios are kept constant. For the WiFi only deployment, we replace all the LTE BSs in Figure 5 with WiFi APs. It is notable that, with the use of MAB, the overall capacity is increased significantly from stand-alone WiFi operation and simultaneous operation of LTE-U and WiFi (without MAB). Also we found that with the increase of intersite distance (ISD) in Figure 5, the

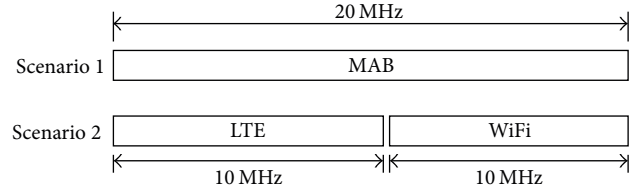


FIGURE 6: Scenario with two cases.

capacity decreases. This is because of higher serving area per APs/STA within the ISDs.

The WiFi throughput performance with and without MAB algorithm is shown in Figure 8, where it is noted that MAB algorithm improves the WiFi throughput over the two other scenarios. Moreover, with the increase of ISD, capacity degrades for all cases. The effect of LTE packet arrival rate on aggregate capacity is shown in Figure 9. We found that the aggregate throughput of coexisting LTE and WiFi networks is maximized for  $\lambda_L = 2.5$ , but then it decreases for larger values of  $\lambda_L$  due to increased interference levels. Also for full buffer LTE traffic ( $\lambda_L = 0$ ), the coexisting system with MAB has degraded performance compared to coexisting system without MAB.

Impact of energy detection threshold on aggregate capacity is shown in Figure 10. It is observed that -62 dBm threshold provides best performance for all scenarios. Sensing threshold less than -62 dBm makes WiFi back off from transmission in the presence of LTE transmission and results in lower aggregate capacity. On the other hand, sensing threshold more than -62 dBm allows WiFi to transmit in the presence of LTE operation, which reduces aggregate capacity due to higher interference.

For Figure 11, we consider a scenario with two cases as described in Figure 6. In scenario 1, we consider simultaneous operation of LTE-U and WiFi using MAB on 20 MHz bandwidth. On the other hand, in scenario 2, stand-alone LTE (i.e., 100% duty cycle) and WiFi are operating on separate 10 MHz bandwidth. We find that the overall capacity using MAB is improved significantly when compared with the aggregate capacity of two stand-alone systems. This reflects how the spectral efficiency can be improved using MAB and motivates sharing of wireless spectrum among LTE and WiFi networks, rather than deploying them separately.

The impact of LTE-U UEs and WiFi STAs density on aggregate capacity is given in Figure 12. We find that the aggregate capacity improves for the reductions of users in both services. Comparatively high sensitivity could be seen when the density of STAs is changed. When the densities are reduced, particularly the STAs, a significant increase in capacity is achieved under reduced interference conditions. However, this reduction is further contributed by the CSMA/CA mechanism as well. Also it is notable that capacity decreases with the increase of ISD.

**5.2. Cell-Edge Performance.** In Figure 13, 5th percentile LTE throughput for different user densities of STAs is represented. We found that with the increase of STAs, 5th percentile UE throughput reduces due to more interference caused by STAs.

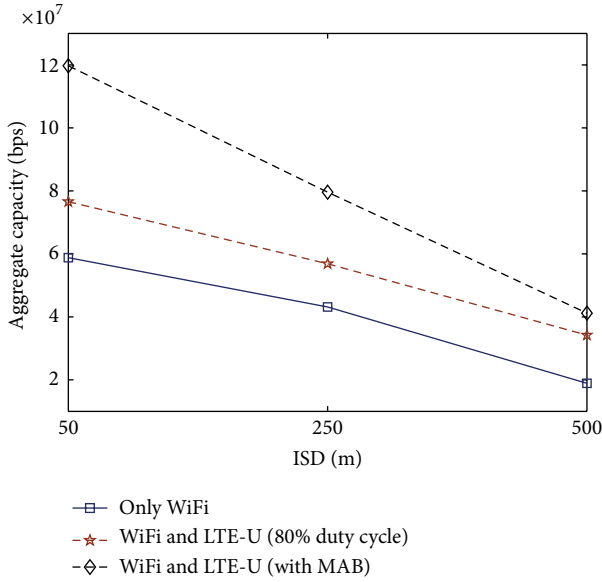


FIGURE 7: Aggregate capacity of coexisting WiFi and LTE-U (80% duty cycle), MAB based coexisting LTE-U and WiFi, and stand-alone WiFi system for different ISDs.

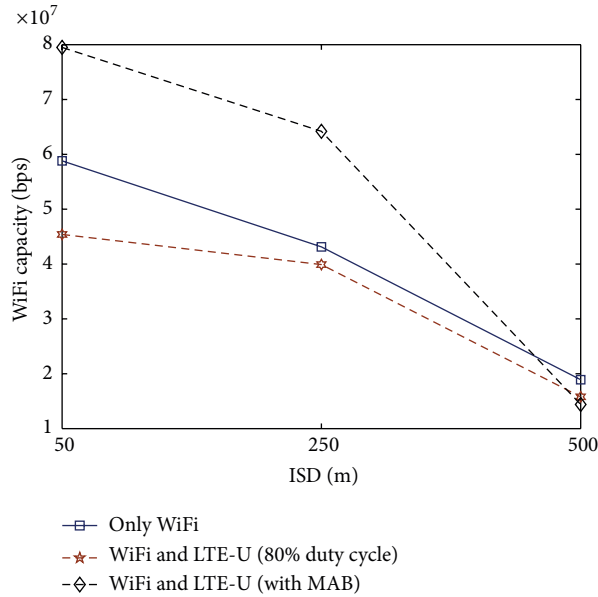


FIGURE 8: WiFi capacity of coexisting WiFi and LTE-U (80% duty cycle), MAB based coexisting LTE-U and WiFi, and stand-alone WiFi system for different ISDs.

However, with the increment of UEs, the effect of STA density reduces. This means that, for higher density of UEs and STAs, fewer LTE users will experience higher capacity.

5.3. *Energy Efficiency Performance.* Aggregate capacity of  $|\mathcal{Q}_L^i| = 10$  and  $|\mathcal{Q}_W^w| = 10$  is presented in Figure 14 for different power control techniques. Four parameter settings are used for PC. In the first instance, no PC is considered. In the second case, PC is used by replacing the parameters in Step (7) of the

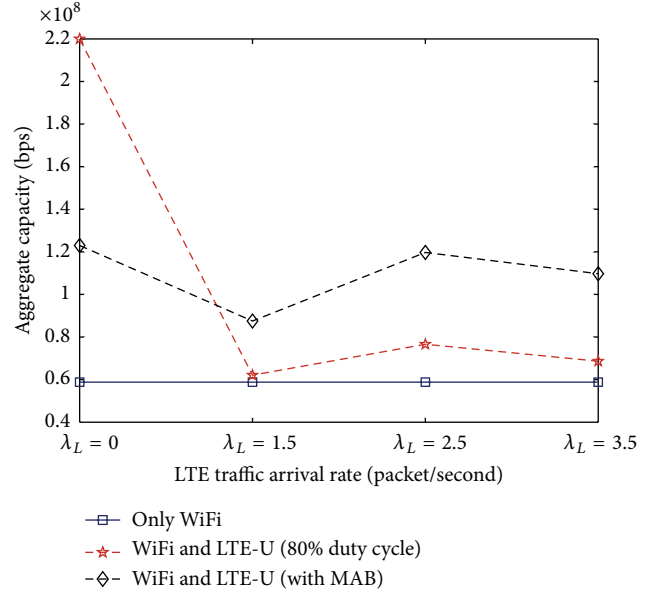


FIGURE 9: Aggregate capacity of coexisting WiFi and LTE-U (80% duty cycle), MAB based coexisting LTE-U and WiFi, and stand-alone WiFi system for different LTE traffic arrival rates.

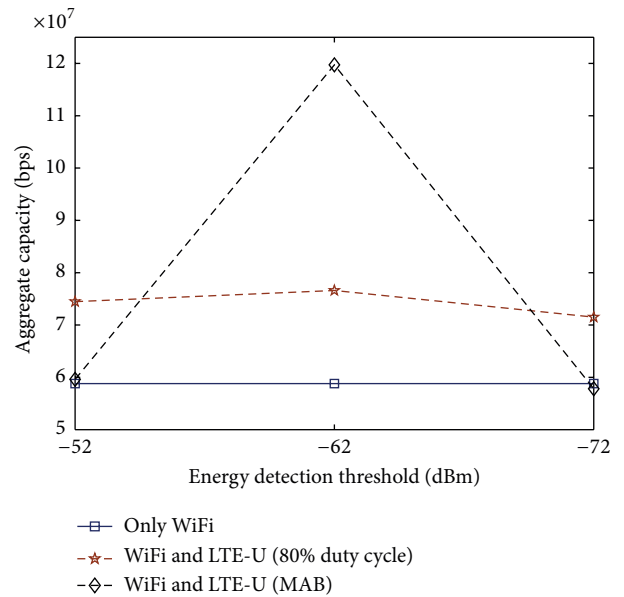


FIGURE 10: Aggregate capacity of coexisting system of WiFi and LTE-U (80% duty cycle), MAB based coexisting LTE-U and WiFi, and stand-alone WiFi system for various energy detection thresholds.

Algorithm 1 with  $C_i/p_s^i > C_j^{\min}/P_{\min}$ , where  $P_{\min} = 8$  dBm. For the third and fourth cases, parameters are replaced with  $C_i/p_s^i > C_j^{\min}/P_{\max}$  and  $C_i > C_j^{\min}$ , where  $P_{\max} = 23$  dBm. The set of power levels is defined as  $\mathcal{P}_i = \{p_1^i, p_2^i, \dots, p_{|\mathcal{P}|}^i\} = \{8, 11, 14, 17, 20, 23\}$  dBm, where  $P_{\min} = 8$  dBm and  $P_{\max} = 23$  dBm. So, in the second and third cases a given level of energy efficiency is aimed at. In the last case, according to the explanation given for (9), the level is dynamically adjusted. It

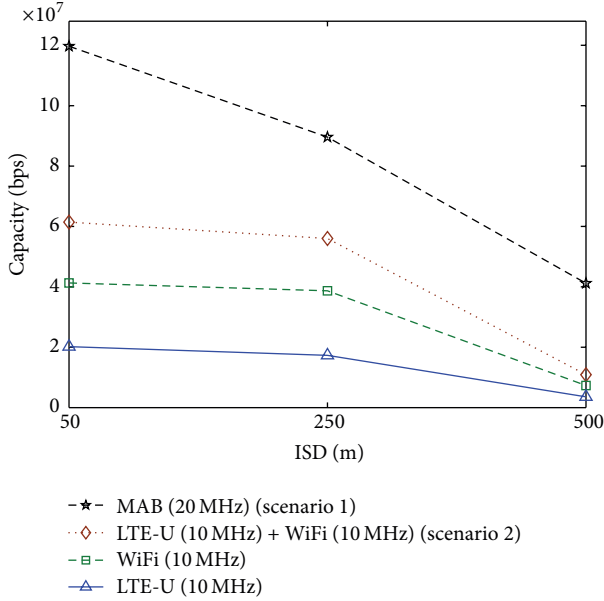


FIGURE 11: Capacity of 10 STAs or/and 10 UEs under stand-alone WiFi, stand-alone LTE, coexisting stand-alone WiFi, and LTE-U (scenario 1) and MAB based coexisting LTE-U and WiFi (scenario 2) for different bandwidths and ISDs.

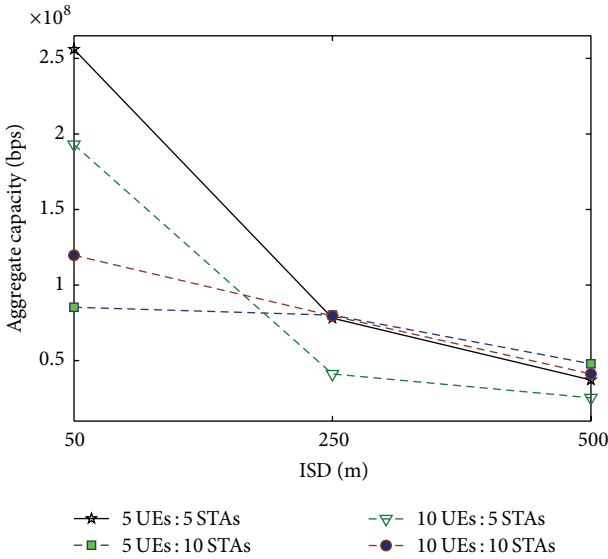


FIGURE 12: Capacity of MAB based coexistence for different UEs and STAs ratios and ISDs.

is noted that the best and worst performances are found for  $P_{\max}$  and  $P_{\min}$ . For MAB with PC, optimum result is found.

In Figure 15, different numbers of UEs are considered to evaluate energy efficiency performance. For all the densities, the least efficiency is achieved with no PC. In the most dense scenario, the best efficiency can be observed under the second configuration,  $C_j^{\min}/P_{\min}$  [see (9)]. As it is expected with the reduction of densities, energy efficiency is increased. However, after a certain average energy efficiency level, no significant improvements could be observed.

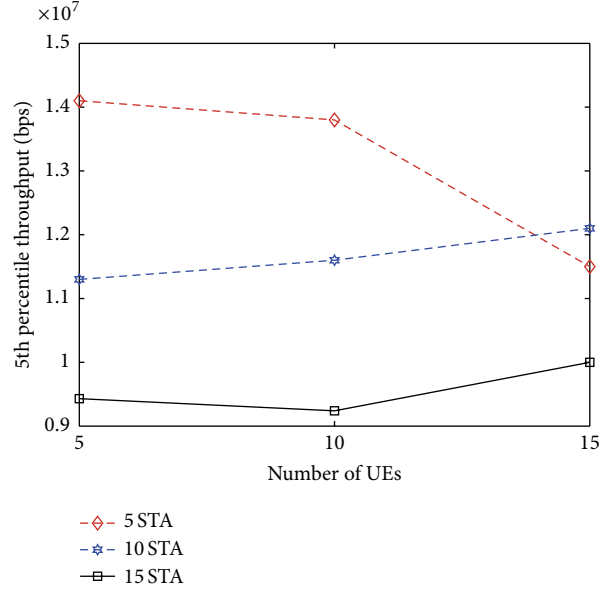


FIGURE 13: 5th percentile throughput of MAB based coexisting LTE-U and WiFi for different UEs and STAs ratios.

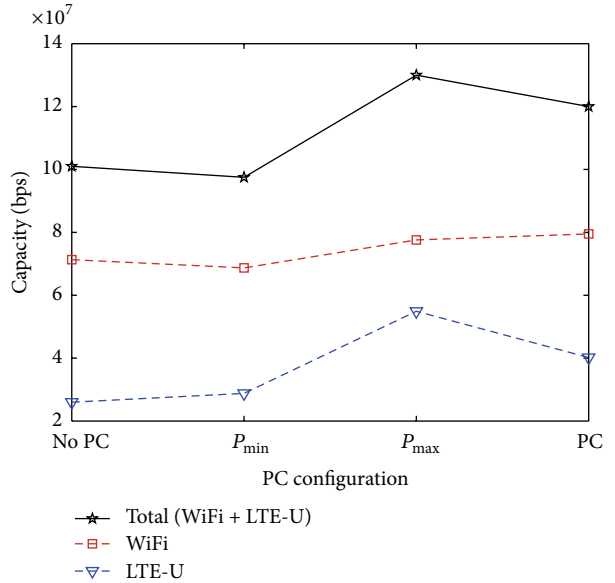


FIGURE 14: Capacity of 10 UEs and 10 STAs under different PC configurations.

## 6. Conclusion

In this paper, a MAB based dynamic duty cycle selection method was proposed to facilitate spectrum sharing between WiFi and LTE-U in the same unlicensed band. Performance of the proposed algorithm was further enhanced by using a DL PC technique. Subsequently, the proposed concept was extended to optimize energy efficiency. Considerable gains in overall throughputs could be achieved via the proposed MAB while ensuring a minimum capacity for LTE-U based services in the same band. Significant gains in terms of energy efficiency could be achieved where it is observed that the

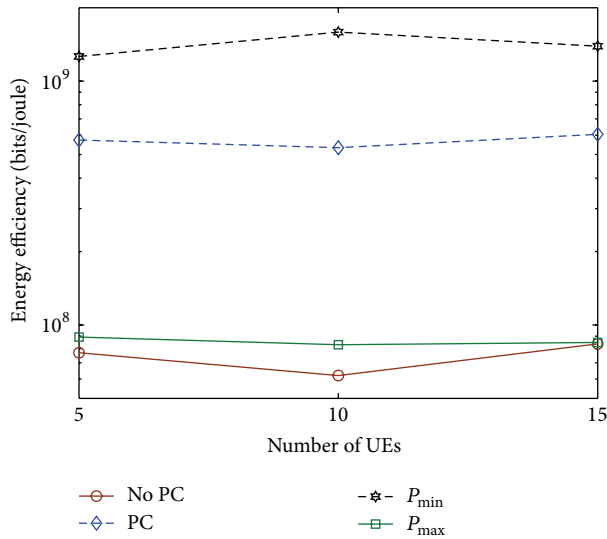


FIGURE 15: Energy efficiency under different PC configurations for various numbers of UEs (with 10 STAs).

gains under different parameter settings with PC are much higher than those with no PC. Our future work includes extending our framework to scenarios with IA and PAL users in the same spectrum.

## Competing Interests

The authors declare that there is no conflict of interests regarding the publication of this paper.

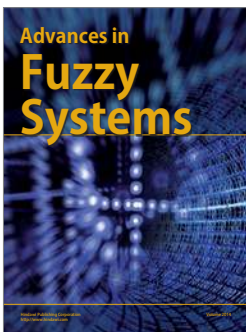
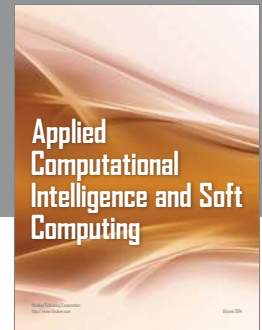
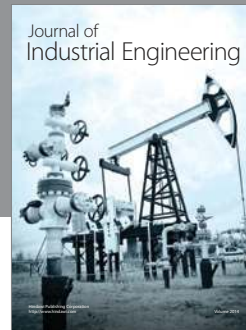
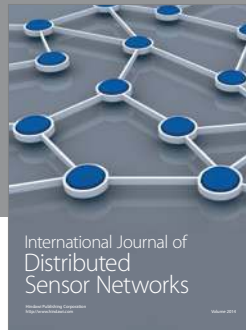
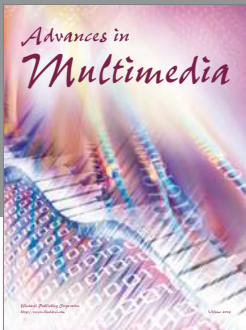
## Acknowledgments

The authors would like to thank Nadisanka Rupasinghe for developing an earlier version of the simulator used in this paper. This research was supported in part by the US National Science Foundation (NSF) under Grants nos. ACI-1541108 and AST-1443999 and Presidential Fellowship under Florida International University.

## References

- [1] NSN Whitepaper, “Enhance mobile networks to deliver 1000 times more capacity by 2020,” Tech. Rep., 2013.
- [2] M. Simsek, M. Bennis, and I. Güvenc, “Enhanced intercell interference coordination in HetNets: single vs. multiflow approach,” in *Proceedings of the IEEE Globecom Workshops (GC Wkshps '13)*, pp. 725–729, Atlanta, Ga, USA, December 2013.
- [3] M. Simsek, M. Bennis, and I. Güvenc, “Learning based frequency- and time-domain inter-cell interference coordination in HetNets,” *IEEE Transactions on Vehicular Technology*, vol. 64, no. 10, pp. 4589–4602, 2015.
- [4] FCC, “Amendment of the commissions rules with regard to commercial operations in the 3550–3650 MHz band,” Notice of Proposed Rulemaking and Order, 2012, [https://apps.fcc.gov/edocs\\_public/attachmatch/DA-15-955A1\\_Rcd.pdf](https://apps.fcc.gov/edocs_public/attachmatch/DA-15-955A1_Rcd.pdf).
- [5] FCC, “Amendment of the commissions rules with regard to commercial operations in the 3550–3650 MHz band,” Report and Order and Second Further Notice of Proposed Rulemaking 12-354, 2015, [https://apps.fcc.gov/edocs\\_public/attachmatch/FCC-15-47A1.pdf](https://apps.fcc.gov/edocs_public/attachmatch/FCC-15-47A1.pdf).
- [6] R. Zhang, M. Wang, L. X. Cai, Z. Zheng, X. S. Shen, and L.-L. Xie, “LTE-unlicensed: the future of spectrum aggregation for cellular networks,” *IEEE Wireless Communications*, vol. 22, no. 3, pp. 150–159, 2015.
- [7] “Study on licensed-assisted access using LTE,” Tech. Rep. RP-141397, 3GPP Study Item, Edinburgh, Scotland, 2014.
- [8] 3GPP, “Study on licensed-assisted access to unlicensed spectrum,” Tech. Rep. TR 36.899, 3GPP, Athens, Greece, 2015.
- [9] L. Cai, X. Shen, J. W. Mark, and Y. Xiao, “Voice capacity analysis of WLAN with unbalanced traffic,” in *Proceedings of the 2nd International Conference on Quality of Service in Heterogeneous Wired/Wireless Networks (QSHINE '05)*, pp. 8–9, Lake Vista, Fla, USA, August 2005.
- [10] F. M. Abinader, E. P. L. Almeida, F. S. Chaves et al., “Enabling the coexistence of LTE and Wi-Fi in unlicensed bands,” *IEEE Communications Magazine*, vol. 52, no. 11, pp. 54–61, 2014.
- [11] I. Parvez, N. Islam, N. Rupasinghe, A. I. Sarwat, and I. Güvenc, “LAA-based LTE and ZigBee coexistence for unlicensed-band smart grid communications,” in *Proceedings of the SoutheastCon 2016*, pp. 1–6, Norfolk, Va, USA, March-April 2016.
- [12] N. Rupasinghe and I. Güvenc, “Licensed-assisted access for WiFi-LTE coexistence in the unlicensed spectrum,” in *Proceedings of the IEEE Globecom Workshops (GC Wkshps '14)*, pp. 894–899, Austin, Tex, USA, December 2014.
- [13] N. Rupasinghe and I. Güvenc, “Reinforcement learning for licensed-assisted access of LTE in the unlicensed spectrum,” in *Proceedings of the IEEE Wireless Communications and Networking Conference (WCNC '15)*, pp. 1279–1284, New Orleans, La, USA, March 2015.
- [14] M. G. S. Sriyananda, I. Parvez, I. Güvenc, M. Bennis, and A. I. Sarwat, “Multi-Armed Bandit for LTE-U and WiFi coexistence in unlicensed bands,” in *Proceedings of the IEEE Wireless Communications and Networking Conference (WCNC '16)*, Doha, Qatar, April 2016.
- [15] T. Ran, S. Sun, B. Rong, and M. Kadoch, “Game theory based multi-tier spectrum sharing for LTE-A heterogeneous networks,” in *Proceedings of the IEEE International Conference on Communications (ICC '15)*, pp. 3033–3038, London, UK, June 2015.
- [16] F. Shams, G. Bacci, and M. Luise, “A Q-learning game-theory-based algorithm to improve the energy efficiency of a multiple relay-aided network,” in *Proceedings of the 31st General Assembly and Scientific Symposium of the International Union of Radio Science (URSI GASS '14)*, pp. 1–4, XXXIth URSI, August 2014.
- [17] J. C. Gittins, “Bandit processes and dynamic allocation indices,” *Journal of the Royal Statistical Society—Series B: Methodological*, vol. 41, no. 2, pp. 148–177, 1979.
- [18] P. Auer, N. Cesa-Bianchi, and P. Fischer, “Finite-time analysis of the multiarmed bandit problem,” *Machine Learning*, vol. 47, no. 2, pp. 235–256, 2002.
- [19] A. M. Cavalcante, E. Almeida, R. D. Vieira et al., “Performance evaluation of LTE and Wi-Fi coexistence in unlicensed bands,” in *Proceedings of the IEEE 77th Vehicular Technology Conference (VTC Spring '13)*, pp. 1–6, Dresden, Germany, June 2013.
- [20] R. Kwan, R. Pazhyannur, J. Seymour et al., “Fair co-existence of Licensed Assisted Access LTE (LAA-LTE) and Wi-Fi in unlicensed spectrum,” in *Proceedings of the 7th Computer Science and Electronic Engineering (CEEC '15)*, pp. 13–18, Colchester, UK, September 2015.

- [21] N. Whitepaper, “Views on LAA for unlicensed spectrum—scenarios and initial evaluation results,” Tech. Rep. RWS-140026, 3GPP RAN1 Standard Contribution, Sophia Antipolis, France, 2014.
- [22] Qualcomm, “Qualcomm research LTE in unlicensed spectrum: harmonious coexistence with WiFi,” Tech. Rep., 3GPP RAN1 Standard Contribution, 2014.
- [23] E. Almeida, A. M. Cavalcante, R. C. D. Paiva et al., “Enabling LTE/WiFi coexistence by LTE blank subframe allocation,” in *Proceedings of the IEEE International Conference on Communications (ICC '13)*, pp. 5083–5088, IEEE, Budapest, Hungary, June 2013.
- [24] T. Nihtila, V. Tykhomyrov, O. Alanen et al., “System performance of LTE and IEEE 802.11 coexisting on a shared frequency band,” in *Proceedings of the IEEE Wireless Communications and Networking Conference (WCNC '13)*, pp. 1038–1043, Shanghai, China, April 2013.
- [25] F. S. Chaves, E. P. L. Almeida, R. D. Vieira et al., “LTE UL power control for the improvement of LTE/Wi-Fi coexistence,” in *Proceedings of the IEEE 78th Vehicular Technology Conference (VTC Fall '13)*, pp. 1–6, September 2013.
- [26] N. Rupasinghe and I. Güvenç, “Licensed-assisted access for WiFi-LTE coexistence in the unlicensed spectrum,” in *Proceedings of the IEEE Globecom Workshops (GC Wkshps '14)*, pp. 894–899, Austin, Tex, USA, December 2014.
- [27] X. Xu, G. Kutrolli, and R. Mathar, “Dynamic downlink power control strategies for LTE femtocells,” in *Proceedings of the 7th Next Generation Mobile Applications, Services and Technologies Conference*, pp. 181–186, September 2013.
- [28] Z. Wang, W. Xiong, C. Dong, J. Wang, and S. Li, “A novel downlink power control scheme in LTE heterogeneous network,” in *Proceedings of the International Conference on Computational Problem-Solving (ICCP '11)*, pp. 241–245, Chengdu, China, October 2011.
- [29] T. Zahir, K. Arshad, Y. Ko, and K. Moessner, “A downlink power control scheme for interference avoidance in femtocells,” in *Proceedings of the 7th International Wireless Communications and Mobile Computing Conference (IWCMC '11)*, pp. 1222–1226, July 2011.
- [30] S. Maghsudi and S. Stanczak, “Channel selection for network-assisted D2D communication via no-regret bandit learning with calibrated forecasting,” *IEEE Transactions on Wireless Communications*, vol. 14, no. 3, pp. 1309–1322, 2015.
- [31] M. Simsek, M. Bennis, and I. Guvenc, “Mobility management in HetNets: a learning-based perspective,” *EURASIP Journal on Wireless Communications and Networking*, vol. 2015, no. 1, article 26, pp. 1–13, 2015.
- [32] R. Combes and A. Proutiere, “Dynamic rate and channel selection in cognitive radio systems,” *IEEE Journal on Selected Areas in Communications*, vol. 33, no. 5, pp. 910–921, 2015.
- [33] G. Locke and L. E. Strickling, “An assessment of the near-term viability of accommodating wireless broadband systems in the 1675–1710 MHz, 1755–1780 MHz, 3500–3650 MHz, and 4200–4220 MHz, 4380–4400 MHz bands,” Report, 2010, <https://www.ntia.doc.gov/files/ntia/publications/fasttrackevaluation.11152010.pdf>.
- [34] P. R. Atkins, “NTIA letter office of engineering and technology, FCC,” GN Docket No. 12-354, 2015, [http://www.ntia.doc.gov/files/ntia/publications/ntia\\_letter\\_docket\\_no\\_12-354.pdf](http://www.ntia.doc.gov/files/ntia/publications/ntia_letter_docket_no_12-354.pdf).
- [35] L. Stefani, “The FCC Raises the Curtain on the Citizens Broadband Radio Service,” *CommLawBlog Article*, May 2015, <http://www.commlawblog.com/2015/05/articles/unlicensed-operations-and-emer/the-fcc-raises-the-curtain-on-the-citizens-broadband-radio-service/>.
- [36] FCC, “3.5 GHz Spectrum Access System Workshop,” Washington, DC, USA, 2014, <https://www.fcc.gov/news-events/events/2014/01/35-ghz-spectrum-access-system-workshop>.
- [37] “RSPG opinion on licensed shared access,” Tech. Rep. RSPG13-538, European Commission, Radio Spectrum Policy Group, 2013.
- [38] ECC, “Licensed shared access,” Tech. Rep. ECC 205, 2014.
- [39] S. Sesia, I. Toufik, and M. Baker, *LTE—The UMTS Long Term Evolution: From Theory to Practice*, John Wiley & Sons, New York, NY, USA, 2009.
- [40] E. Perahia and R. Stacey, *LTE: The UMTS Long Term Evolution, From Theory to Practice*, Cambridge University Press, New York, NY, USA, 2008.
- [41] S. Agrawal and N. Goyal, “Analysis of thompson sampling for the multi-armed bandit problem,” <https://arxiv.org/abs/1111.1797>.
- [42] N. Gupta, O.-C. Granmo, and A. Agrawala, “Thompson sampling for dynamic multi-armed bandits,” in *Proceedings of the 10th International Conference on Machine Learning and Applications (ICMLA '11)*, vol. 1, pp. 484–489, Honolulu, Hawaii, USA, December 2011.
- [43] P. Auer, N. Cesa-Bianchi, and P. Fischer, “Finite-time analysis of the multiarmed bandit problem,” *Machine Learning*, vol. 47, no. 2-3, pp. 235–256, 2002.
- [44] J. Langford and T. Zhang, “The epoch-greedy algorithm for multiarmed bandits with side information,” in *Advances in Neural Information Processing Systems*, J. C. Platt, D. Koller, Y. Singer, and S. T. Roweis, Eds., vol. 20, pp. 817–824, Curran Associates, 2008.
- [45] 3GPP, “Evolved Universal Terrestrial Radio Access (E-UTRA); further advancements for E-UTRA physical layer aspects (release 9),” Tech. Rep. TR36.814, V9.0.0, 3GPP, 2010.



**Hindawi**

Submit your manuscripts at  
<http://www.hindawi.com>

